

# Tectonic and Geodynamic Evolution of the Northern Australian Margin and New Guinea

\***Joanna Tobin**  
University of Sydney  
NSW 2006  
jotobin@gmail.com

**Dr. Sabin Zahirovic**  
University of Sydney  
NSW 2006  
sabin.zahirovic@sydney.edu.au

**Dr. Rakib Hassan**  
Geoscience Australia  
Symonston ACT 2609  
rakib.hassan@ga.gov.au

**A/Prof. Patrice Rey**  
University of Sydney  
NSW 2006  
patrice.rey@sydney.edu.au

\*presenting author asterisked

## SUMMARY

Rapid convergence between the Indo-Australian, Southeast Asian, and Pacific plates in the Cenozoic has resulted in a complex tectonic evolution of Australia's northern margin. A lack of available geologic data leads to large uncertainties, such as the timing of the Sepik collision with the New Guinea margin, currently constrained to sometime between 50 and 30 Ma. Previous work suggested a link between the Sepik collision and a voluminous fast seismic anomaly presently in the mantle beneath Lake Eyre. Following from previous work, this study uses coupled plate reconstruction and numerical geodynamic models to test 50 Ma and 30 Ma collision timings of the Sepik terrane, along with an upper extent back-arc basin, to further refine our understanding of the origin and trajectory of the slab beneath Lake Eyre and address uncertainties in the plate reconstructions. The results of mantle flow models indicate that the Eocene collision timing (~50 Ma) is more likely than an Oligocene collision (~30 Ma). In addition, dynamic topography results support previous suggestions that dynamic subsidence relating to the down-going Sepik slab has influenced the evolution of the Eyre Basin, with up to ~100 m of dynamic subsidence since ~20 Ma. However, further work is required to address numerical issues relating to rapid thermal diffusion of slab material, and to investigate reasonable trench retreat velocities for intermediate (~3000 km) subduction zone lengths. This work highlights the role of numerical experiments in understanding transient plate-mantle processes and their effect on basin evolution.

Key words: New Guinea, Australia, plate tectonic reconstruction, seismic tomography, dynamic topography.

## INTRODUCTION

The northern margin of the Australian plate has evolved through the long-term convergence between the Indo-Australian, Eurasian and Pacific plates during Pangea dispersal. The tectonic history of this margin has recorded episodes of basin opening, which have since been consumed by subduction, with the only traces of geological evidence recorded in the obducted ophiolites and accreted volcanic arcs (Fig. 1). This complex tectonic history has been the subject of a wide range of studies spanning decades (e.g. Dow, 1977; Pigram and Davies, 1987; Hill and Hall, 2003; Baldwin et al., 2012), however, much of this history remains uncertain due to an absence of preserved seafloor spreading constraints, as well as a scarcity of geologic data as a result of extensive weathering and large regions of inaccessible terrain. Further constraints on the timing and nature of tectonic events in northern New Guinea is needed to provide a deeper understanding of the evolution of the margin, and help connect the tectonic reconstructions between the western Pacific, the Indian Ocean and Southeast Asia, as well as to provide greater insight into the development of key economic resources throughout the region. Of particular interest is the timing of the collision between the Sepik terrane and the former passive northern margin of the Australian plate, with collision currently loosely constrained to between ~50 and 30 Ma. This study aims to constrain the timing of this collision by using plate reconstruction software GPlates and mantle flow numerical modelling code CitcomS to test two end-member scenarios. In addition, this study computes the dynamic topography for each end-member scenario, in order to investigate the influence that the closure of the Sepik back-arc basin and the down-going Sepik slab has on the long wavelength topography of the Australian continent. These geodynamic models can also provide insight into the size of the oceanic gateway between the Sepik terrane and New Guinea, of which only slivers of ophiolite remain in the suture zone. Along with understanding the timing of ocean basin openings and closures, constraining the size of oceanic gateways can provide a greater understanding of paleo-ocean circulation, sea level and climate changes, as well as biological dispersal pathways. Zahirovic et al. (2016) investigated a small end-member for the size of this gateway, and building on these results, this study will investigate other scenarios that aim to reconcile the surface geology and the deep mantle structure.

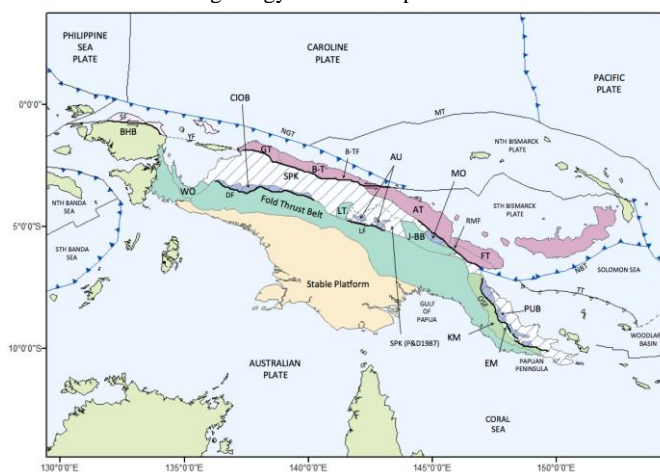


Figure 1: Regional geology based on Baldwin et al. (2012), Hill and Hall (2003), Pigram and Daves (1987), Zahirovic et al. (2016), representing major tectonic regions and features: AT = Adelberg terrane, AU = April Ultramafics, BHB = Bird's Head Block, B-T = Bewani-Torricelli terrane, B-TF = Bewani-Torricelli fault zone, CIOB = Central Irian Ophiolite Belt, DF = Derewo fault, EM = Emo Metamorphics, FT = Finisterre terrane, GT = Gautier terrane, J-BB = Jimi Bena Bena terrane, KM = Kagi metamorphics, LF = Lagaip fault, LT = Landslip terrane, MO = Marum Ophiolite, MT = Manus Trench, NBT = New Britain Trench, NGT = New Guinea Trench, OSF = Owen-Stanly fault zone, PUB = Papuan Ultramafic Belt, RMF = Ramu-Markham fault, SF = Sorong fault zone, SPK = Sepik terrane, SPK (P&D 1987) = Sepik terrane as originally defined in Pigram and Davies (1987), TT = Trobriand Trough, WO = Weyland Overthrust, YF = Yapen fault zone. Pink terranes = accreted volcanic arcs of the Melanesian arc collision.

Constraints on the timing of the collision between the Sepik terrane and the former passive northern margin of the Australian plate suggest two potential end-members of ~50 Ma and ~30 Ma. Evidence suggesting a collision close to 50 Ma includes the ~58 Ma  $^{40}\text{Ar}/^{39}\text{Ar}$  amphibole ages of the metamorphic sole of the Papuan Ultramafic Belt (PUB), which Lus et al. (2004) infers to suggest a ~51-57 Ma age of obduction, and Schellart and Spakman (2015) which discusses the potential for the collision to be related to the termination of spreading in the Coral Sea ~52 Ma (Gaina et al., 1999). Spreading between the northeast of Australia, Papuan Plateau/Peninsula occurred between 63-52 Ma (Gaina, 1999), and Schellart and Spakman (2015) suggests that the cessation of this spreading may be contemporaneous with the collision of the Sepik terrane and the termination of subduction. Plate reconstruction constraints in the broader region do not allow for the collision and termination of subduction to have occurred prior to the cessation of Coral Sea spreading, hence ~50 Ma forms a maximum age for the docking of the Sepik terrane with the New Guinea margin. Authors who have suggested a ~50 Ma collision for the Sepik terrane include Hall (1996; 2002; 2012), Lus et al. (2004), and Schellart and Spakman (2015). A 30 Ma collision end-member is suggested in two particular sets of geological data. In central New Guinea K-Ar metamorphic cooling ages of 27-23 Ma relate to exhumation during extension, which Crowhurst et al. (1996) infer to be related to post collisional slab rollback, suggesting collision timing of ~30 Ma. In addition to this, the Ar-Ar dating of the Emo metamorphics on the Papuan Peninsula, yielding dates of 35-31 Ma, are interpreted by Worthing and Crawford (1996) to relate to contemporaneous emplacement of the PUB. As these are the youngest dates relating to the Sepik collision, they form the younger end-member for docking with the New Guinea margin. Authors who suggest a 30 Ma Sepik collision include Zahirovic et al. (2016), Klootwijk et al. (2003), and Worthing and Crawford et al. (1996).

This study has three primary aims. The first is to gain greater insight into the timing of the collision between the Sepik terrane and the northern margin of the Australian plate through testing two end-member collision scenarios. The second is to explore an upper end-member size of the Sepik back-arc basin, and the third to investigate the effect the Sepik slab has on the long wavelength topography of the Australian continent. Our strategy was to design two plate reconstruction models, one for each end-member collision timing of 50 and 30 Ma, with both of these incorporating an upper end-member size of the Sepik back-arc basin (~3000 km). Each plate model acts as surface boundary condition in the numerical mantle convection code, and the results of forward geodynamic experiments is investigated through comparison with P- and S-wave seismic tomography models. Dynamic topography is computed from the time dependent output of these models.

Zahirovic et al. (2016) has explored this margin through forward geodynamic experiments investigating a ~30 Ma collision and a small end-member Sepik back-arc basin (~500 km width). Due to the uncertainties in the plate reconstructions for this region, this study explores the larger end-member size for this oceanic basin. The results of the experiments by Zahirovic et al. (2016) link the down-going Sepik slab to a present day fast seismic anomaly beneath Lake Eyre, interpreted in P- and S- wave seismic tomography models. These results indicate a reasonable latitude and depth for the predicted Sepik slab when compared to the fast seismic anomaly, however, the thermal anomaly related to the slab is quite small (Fig. 2). The results open up the possibility for both an earlier timing of collision, as well as a larger back-arc basin. Due to both a lack of constraints on the size of the Sepik back-arc basin, as well as the scarcity of evidence relating to the timing of the Sepik collision, employing end-member scenarios becomes an important tool in addressing the uncertainties in the plate reconstructions.

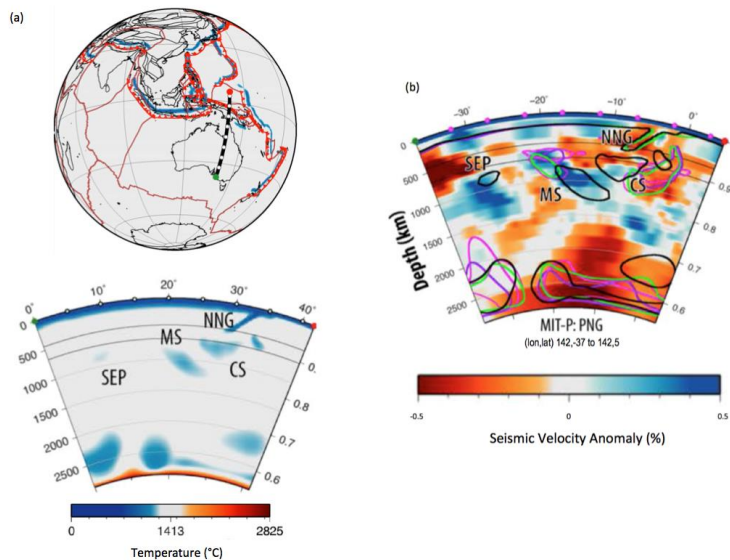


Figure 2: (a) Numerically modelled Sepik slab (SEP) based on a small end-member oceanic gateway. (b) the contour of the Sepik slab plotted over seismic tomography (Li et al. (2008) MIT-P08) – this is relatively small when compared to the fast seismic anomaly at 30°S, however indicates a reasonable depth and latitude. From Zahirovic et al. (2016).

Schellart and Spakman (2015) independently linked the down-going Sepik slab to this same fast seismic anomaly beneath Lake Eyre. This work investigates the influence that the Sepik slab has on the dynamic topography of the Australian continent, and suggests that the down-going slab is directly related to the topographic depression associated with Lake Eyre. Schellart and Spakman (2015) assumes a 50 Ma collision timing of the Sepik terrane with the New Guinea margin, and the dynamic topography is explored through a Cartesian box setup assuming vertical sinking of a slab in a pristine and idealized mantle. This study will compute time dependent dynamic topography for each of the 50 and 30 Ma end member models, investigating this in a global geodynamic setup, and assess the effect each model has on the long wavelength topography of the Australian continent.

## METHOD AND RESULTS

### Methods

Due to the lack of preserved seafloor spreading history for the now-subducted Sepik back-arc basin, alternate methods need to be employed for the reconstruction of this region. End-member scenarios for the evolution of this margin are constructed using a synthesis of regional geology, and to capture the uncertainties in the timing of the Sepik collision with the New Guinea margin, two end-member scenarios of ~50 and ~30 Ma for the timing of this accretion are implemented. These plate reconstructions are applied as surface boundary conditions to numerical mantle flow models, whose predictions of slab distributions are qualitatively compared to fast seismic velocities in P- and S-wave seismic tomography. The time dependent dynamic topography from the geodynamic models is also computed to infer the influence of the subduction history on the long-wavelength topography of the Australian continent. These methods combine geological constraints from the surface, along with previously underutilized constraints from the deep Earth, to help address some of the major uncertainties in the tectonic evolution of a complex region, that links the Pacific and Tethyan realms, and with major consequences for ocean circulation, climate, ore emplacement and hydrocarbon generation.

#### Plate tectonic reconstructions:

In creating the plate reconstruction models, this study uses the Zahirovic et al. (2016) scenario for the New Guinea region as a base model. This base model is modified to test the potential north-south extent of the Sepik back-arc basin, and also to test alternative timings of the collision between the Sepik terrane and New Guinea. Constraints on the upper end-member extent of the Sepik back-arc are based on Philippine Arc paleo-latitude data from Balmater et al. (2015) and Queano et al. (2007) (Fig. 3), as well as kinematic constraints implemented for both 30 Ma and 50 Ma collision models.

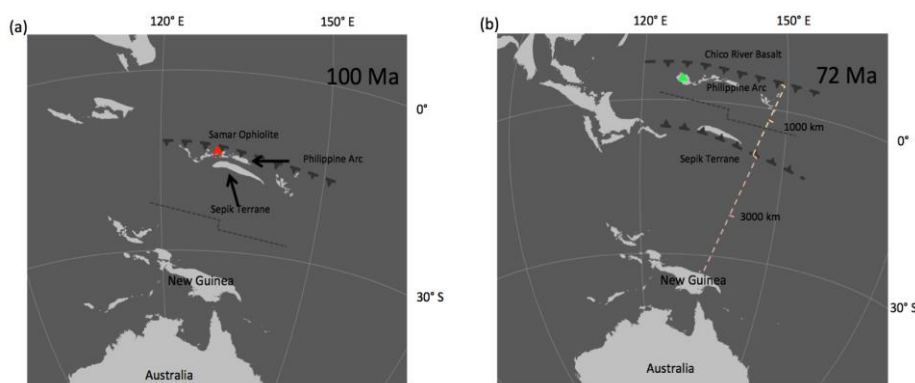


Figure 3: (a) Red triangle = Samar ophiolite paleolatitude data of  $\sim 14^{\circ}\text{S} \pm 6^{\circ}$  at  $\sim 100$  Ma (Balmater et al., 2015), placing a constraint on the maximum opening of the Sepik back-arc basin by this time, and (b) green triangle = Chico River basalt paleolatitude data constraint of  $\sim 6^{\circ}\text{N} \pm 3^{\circ}$  at  $\sim 72$  Ma (Queano et al., 2007). Due to the opposing subduction zones at this time, spreading between the Sepik terrane and the Philippine Arc is initiated at 80 Ma, to ensure numerical errors are avoided when the plate model is coupled with the geodynamic code. The resulting conservative estimate on the upper end-member basin size is  $\sim 3000$  km.

To create the plate models, open source plate reconstruction software GPlates is used, as outlined in Zahirovic et al. (2016). This regional model is embedded in a global set of rotations based on Seton et al. (2012) and refined by Müller et al. (2016), which models plate reconstructions back to 230 Ma, a time of the Pangea supercontinent. Relative motion between plates is implemented using Euler pole rotations, and takes into consideration the relative motion of both the continental blocks, and the oceanic crust associated with each plate. The reconstruction of post-Pangea breakup in the global model is primarily based on sea floor spreading data from the Global Seafloor and Magnetic Lineation Database (Seton et al., 2014), with the relative direction of spreading inferred through fracture zone trends (Matthews et al., 2011; Zahirovic et al., 2016), and the velocity of spreading is calculated via correlation with the Gee and Kent (2007) timescale. This relative spreading history is represented via a set of isochrons and described by finite rotations. In reconstructing synthetic oceanic basins where there is no seafloor spreading data available, such as the Sepik back-arc basin, isochrons are created based on the geological and geophysical data available relating to basin opening and closure timings. The isochrons are used to create a seafloor age grid in 1 Myr intervals from 230 Ma to the present. The age grid is an important aspect of the model, which is used as surface boundary conditions for the geodynamic simulations, providing the reconstructed thermal ages used to calculate the thermal thickness of the seafloor (Flament et al., 2014). The spreading of the Sepik back-arc basin is calculated assuming symmetrical seafloor spreading, and the position of the mid-oceanic ridge is derived from half stage rotations.

The relative plate motion is reconstructed in a hierarchical system linking back to Africa, with Africa then connecting to a reference frame allowing the plate reconstructions to be linked to the underlying mantle and the Earth's spin axis. In this hierarchical system each plate moves relative to another plate higher up in the chain - for example, the Sepik terrane is reconstructed relative to the Australian plate, with the Australian plate moving relative to East Antarctica, which moves relative to Africa. For the fixed, or absolute reference frame, Müller et al. (2016) uses a moving hotspot reference frame (Torsvik et al., 2008) for 70 Ma and younger times. For ages 105 Ma and prior, a True Polar Wander paleomagnetic reference frame (Steinberger and Torsvik, 2008) is implemented, with a 105-70 Ma transition between the two, where a 10 degree longitudinal shift of the paleomagnetic reference frame is used following Butterworth et al. (2014) and van der Meer et al. (2010). GPlates functionality ensures the entire surface of the globe is covered with a set closed plate topologies representing individual tectonic plates in 1 Myr intervals (Gurnis et al., 2012). This enables plate velocities, and subduction zone locations and polarities to be extracted for use as kinematic surface boundary conditions with the geodynamic code.

#### Geodynamic Models:

The geodynamic experiments are run using finite element mantle convection software CitcomS (Zhong et al., 2000). The model is set up in a spherical mantle shell domain, from the core mantle boundary (CMB, ~2800 km depth) to the surface, which is scaled to a non-dimensional Earth radius of 0.55 to 1. The resolution of the model is ~ 50 km at the surface and ~ 28 km at the CMB in the horizontal direction. In the vertical direction there is greater resolution close to the surface (~ 15 km) and the CMB (~30 km), with ambient mantle resolution of ~100 km. Over geologic timescales the mantle is considered to behave as a viscous fluid, and is modelled by governing equations for the conservation of mass, momentum and energy. This study applies CitcomS to perform two sets of thermochemical convection experiments, solving for these equations. The first set of experiments uses the Boussinesq approximation parameterized following Flament et al. (2014), and the second, the extended Boussinesq approximation parameterized following Hassan et al. (2016). The extended Boussinesq approximation (EBA) models pseudo-compressibility of the mantle, with depth-dependent material properties varied through extra terms in the energy equation. The Boussinesq approximation (BA) models incompressible flow, assuming the density remains constant, with only slight variations in density due to temperature allowing for mantle convection.

The temperature field is non-dimensionalised, with the core mantle boundary given a value of 1 and the surface a value of 0. The EBA models have an adiabatic thermal gradient, with the ambient temperature increasing with depth from 0.4 to 0.6, and the top and bottom thermal boundary layers each have a 1225 K (0.4) change in temperature. For the BA models, the ambient mantle is 0.5. Internal heating is applied in the EBA models (absent in the BA models), and the depth-dependent thermal expansivity for the EBA models is computed based on Tosi et al. (2013), while in the BA models the thermal expansivity is not depth dependent. Viscosity and all parameters for the EBA models follow Hassan (2016), and for the BA models follow the setup of Zahirovic et al. (2016).

In coupling the plate reconstruction models with the mantle convection code, a process of “lithospheric assimilation” is performed following the method of Bower et al. (2015). The thermal age of the reconstructed plates determines the thickness of the lithosphere and thermal profile of the upper thermal boundary layer, with the thermal age of the oceanic lithosphere is calculated based on the seafloor age grid representing the age of formation of the lithosphere. Continental lithosphere is divided into three regions representing tectonothermal age (Artemieva, 2006), with thermal ages assigned based on whether the region is Archean, Proterozoic, or Phanerozoic. This global set of reconstructed thermal ages determines the thickness and the thermal profile of the lithosphere based on the half space cooling method, as summarized in Flament et al. (2014). Plate velocities from the plate reconstruction model are extracted in 1 My intervals, and are used as the kinematic surface boundary conditions, placing surface constraints on the mantle convection. Downwellings in the mantle are initiated at convergent plate boundaries (at the locations of paleo-subduction zones) (Bower et al., 2015), and a free slip kinematic boundary condition is applied at the lower thermal boundary layer.

The imposed subduction of lithosphere at convergent plate margins into the mantle involves a process of slab assimilation to a maximum depth of 350 km. This assimilation places constraints on the downgoing slab, including an imposed default slab dip of 45° (that can be varied in the plate reconstructions), a radius of curvature, as well as an average sinking velocity. The thermal structure of the downgoing lithosphere, determined by the seafloor age of the slab, is assimilated according to the methods described in Bower et al. (2015). Below 350 km, the slab is no longer bound by these constraints, and is modelled according to the governing equations driving mantle convection. As an initial condition at 230 Ma, the lithospheric slabs are given an imposed initial depth of 1400 km, with an initial dip of 45° to a depth of 425 km, below which the dip is 90°. Subduction zones, the thermal lithosphere and plate velocities from the plate reconstructions are assimilated at 1 Myr intervals. The models are run from 230 Ma forward to the present day, with output generated at 5 Myr intervals. The output at each interval is used for computing the dynamic topography, and the predicted thermal structure of the mantle at the present is used for comparison with seismic tomography models. Both the 50 Ma and 30 Ma Sepik collision models are run with both EBA and BA. In addition to this, the Zahirovic et al. (2016) model is re-run for both of these setups to ensure fair comparison.

#### Dynamic topography:

Dynamic topography is computed from the output from the geodynamic models. For this calculation, both the EBA and BA mantle flow models are used, and the dynamic topography is calculated following Flament et al. (2014). This is calculated by solving the Stokes equation for each set of output data. For this there is a no slip surface boundary condition, while imposing a free-slip boundary condition at the surface to eliminate influences of traction induced by kinematic plate velocities. We also exclude buoyancy in the top 350 km to exclude influences of data assimilation. The dynamic topography is calculated by scaling the radial stress ( $\sigma'_{rr}$ ) through:

$$h = \frac{\eta_0 \kappa}{\Delta \rho g_0 R_0^2} \sigma'_{rr}$$

where  $\eta_0$  is the reference viscosity,  $\kappa$  the thermal diffusivity,  $\Delta \rho$  density,  $g_0$  gravitational acceleration, and  $R_0$  the Earth's radius. The dynamic topography calculated here represents the vertical component of topography that is related to mantle flow at depths greater than 350 km, and does not capture the role of sub-lithospheric shallow mantle convection, nor the role of plumes in the BA experiments, which are suppressed.

#### Seismic Tomography:

A number of different P- and S-wave models are investigated for this study. As the slab relating the Sepik back-arc basin is under the Australian continent, there is a focus on higher-resolution P-wave models, as these tend to have a higher resolution over continental regions (Becker and Boschi, 2002). As an initial comparison tool the MIT-P08 P-wave model of Li et al. (2008) is used. This model

has a wider global network of data, which includes the Chinese Seismographic Network stations, and is the primary model used for analysis of the Sepik back-arc slab by Zahirovic et al. (2016).

## Results:

The thermal output of the numerical models is examined through a series of vertical slices created perpendicular to the strike of the Sepik subduction zone, capturing the Jurassic-Cretaceous back-arc spreading (~160 Ma), basin closure (~71 Ma), and incorporating the present day Lake Eyre depocenter. This output is generated in 5 Myr intervals with results focused on 160-0 Ma, from the initiation of Sepik back-arc spreading to the present. The vertical slices are used to estimate the sinking rate of the Sepik slab, as well as slab advection trajectories to assess the extent of lateral motion of the slab in the mantle. Present day output has been compared to a number of P- and S-wave seismic tomography models, and is presented here against MIT-P08 P-wave model (Li et al., 2008) (Figure 4). Dynamic topography is examined both regionally and along profiles through the Lake Eyre depocenter via time dependent elevation output at 5 Myr intervals.

### Geodynamic models:

The output of the EBA mantle flow setup displays a comparable evolution of the Sepik slab to the BA models (including re-runs of the Zahirovic et al. (2016) setup). As the EBA models incorporate more of the known properties of the deep mantle, these results are the focus for this presentation. The 30 Ma collision model produced a Sepik slab that was further north in the mantle than the Zahirovic et al. (2016) model (Figs. 2 and 4). The primary difference between these models is the size of the back-arc basin, and although the two models have different slab volumes (due to the different extents of the back-arc basins), the dissimilarities in the slab latitude and geometry at present day largely reflects the strong influence the basin closure velocity has on the evolution of the slab in the mantle. The draping and dragging of slab material along the top of the transition zone in the 30 Ma collision model produces a flattening effect, evident in the present day slab geometry. However, the sub-vertical sinking of the Sepik slab through the transition zone in the Zahirovic et al. (2016) model produces slight folding or buckling of the slab. At the point of slab breakoff, the 30 Ma collision model is not as far south in the mantle as the Zahirovic et al. (2016), largely due to influence of the draped material. This results in the Sepik slab in the 30 Ma collision model 5-10° further north than the Zahirovic et al. (2016) model, illustrating that irrespective of slab breakoff time, the trench velocity can have a significant influence on the final latitude of the slab.

In order to produce a slab both further south than the 30 Ma collision model and larger than the Zahirovic et al. (2016) model, it is likely that slab breakoff would need to occur earlier, when Australia is further south. The results of the 50 Ma collision in EBA mantle flow suggest that this collision timing may be able to produce a slab which correlates well with the fast seismic anomaly beneath Lake Eyre. This result is based on remnant draped slab material that persisted in the mantle slightly further north than the predicted location of slab breakoff (highlighted in the mantle with an adjusted contour in Figure 4). Further investigation of a 50 Ma collision model is required addressing the thermal dissipation of the slab, as well as penetration of the slab into the transition zone. The primary difference between these two models and Zahirovic et al. (2016) is the rapid trench retreat velocity in the closure of the back-arc basin, particularly in the 50 Ma model. Trench retreat velocities in the 50 Ma model are almost double those in the 30 Ma model, and although these are within a reasonable range (when compared to present day trench retreat velocities), they are at the upper end of this range.

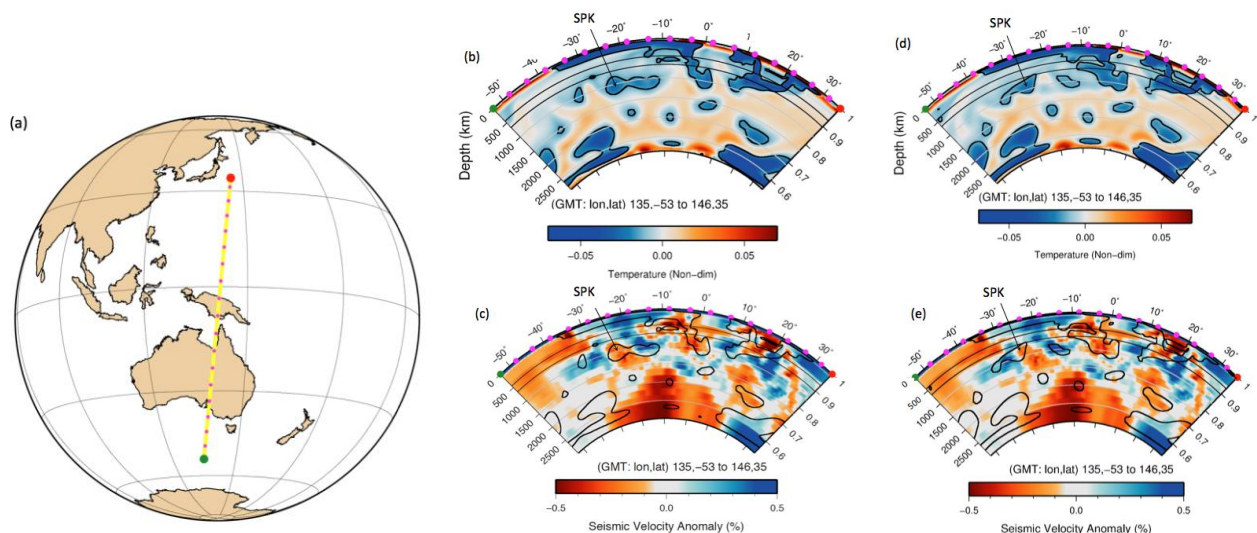


Figure 4: (a) Great circle profile for the modelled present day thermal output, and seismic tomography (b) 30 Ma collision EBA at 0 Ma, with the contour used to define the slab is  $-0.015$  non-dimensional temperature deviation at each depth. (c) MIT-P08 P-wave seismic tomography. The slab from the 30 Ma collision in this setup is too far north at 0 Ma for comparison with the target fast seismic velocity anomaly. (d) 50 Ma collision EBA model at 0 Ma, with the contour used to define the slab is  $-0.0125$  from the deviation at each depth. This contour is slightly warmer temperature than the contour used in the 30 Ma collision model as it is being used to highlight some of the slab material that was “draped” at the transition zone, eventually sinking into the mantle, with the majority of the Sepik slab dissipating soon after slab breakoff. (e) MIT-P08 P-wave seismic tomography. The remnant “draped” Sepik material from the 50 Ma collision in this setup is a better fit at 0 Ma than the slab in the 30 Ma collision model. Given this material was dragged along the transition zone, it is potentially still too far north, and further investigation of a 50 Ma model could produce results with a closer match. SPK = Sepik lithospheric slab

### Dynamic Topography:

The dynamic topography is computed for both the 30 Ma and 50 Ma collision models, as well as the Zahirovic et al. (2016) scenario, calculated based on both the EBA and the BA mantle flow models, using air-loaded scaling (here just the EBA results are presented). The dynamic topography output is presented along great circle profiles incorporating the Sepik subduction zone as well as the present day Lake Eyre depocenter (Fig. 5). In addition, the time-dependent dynamic topography is extracted from two points; one in New Guinea, and the other Lake Eyre (Fig. 6).

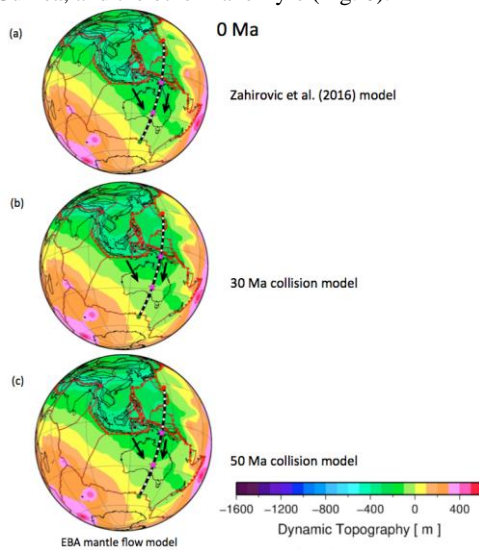


Figure 5: Dynamic topography at 0 Ma for EBA mantle flow models, with arrows indicating the direction of dynamic subsidence. (a) Zahirovic et al. (2016) models, (b) 30 Ma collision models, and (c) 50 Ma collision models.

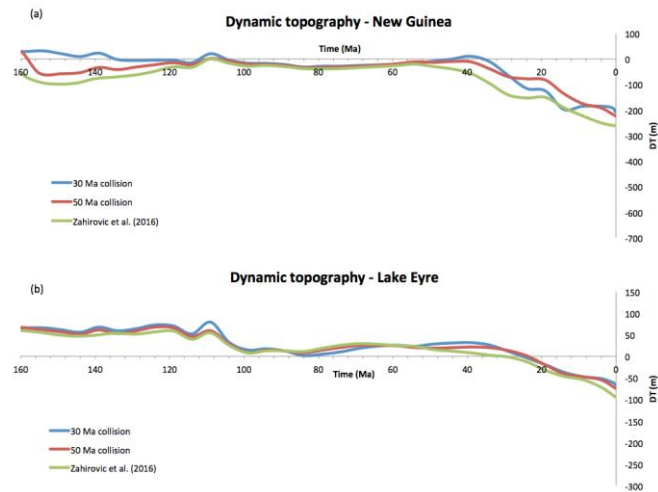


Figure 6: (a) EBA model dynamic topography for New Guinea (location in Fig. 5), indicating dynamic subsidence for the past ~40 Ma, with subsidence initiated in Zahirovic et al. (2016) earlier than in the 30 Ma and 50 Ma collision models due to the close proximity of the Sepik subduction zone to the New Guinea margin (small end-member back-arc basin). (b) Dynamic topography for the Lake Eyre region, indicating subsidence over the past ~20 Myrs in all three EBA models.

As the northward moving Australian plate converges with Southeast Asia there is significant dynamic subsidence visible in all models, and in particular from ~20 Ma, relating to the north-down south-up tilting of Australian continent reflected in the asymmetry of Miocene marine sedimentation (Sandiford, 2007, DiCaprio et al., 2009). All three EBA models show dynamic subsidence in the Eyre Basin region over the past 20-25 Ma.

## CONCLUSIONS

To match the size of the subducted Sepik slab beneath Lake Eyre, the numerical experiments indicate that a ~50 Ma collision of the Sepik terrane with the New Guinea margin is more likely than a ~30 Ma collision scenario. Zahirovic et al. (2016) established a good fit between the Sepik slab and the anomaly, incorporating a small back-arc basin (~500 km) and 30 Ma collision time, however, the slab volume is underestimated. The models in this study incorporating a large extent back-arc basin (~3000 km north-south) require much faster trench retreat velocities (>12 cm/yr), which affects both the evolution of the slab geometry and the sinking trajectory. Rather than sub-vertical sinking through the transition zone (as occurs in the Zahirovic et al. (2016) model), the faster trench retreat velocities result in the slab material being draped along the transition zone, resulting in an elongated geometry when the material enters the lower mantle, and a final position (in the case of these models) further north in the mantle. Hence, the 30 Ma collision model incorporating a wider back-arc basin produced a slab in the lower mantle that fits better with the seismic tomography anomaly, however, it was predicted too far north. In order to produce an equivalent slab further south, slab breakoff would need to occur with Australia further south, hence an earlier collision time is required. The ~50 Ma collision model suggests a much closer fit, however, further work is required to address numerical issues relating to rapid thermal diffusion, and to investigate reasonable trench retreat velocities for intermediate (~3000 km) subduction zone lengths. To overcome the problem of the trench retreat velocity, narrower back-arc basin can be investigated (e.g. 1500-2500 km) with higher numerical model resolutions. It is also important to note, however, that we are comparing thermal and seismic anomalies where there can be smearing involved.

Results of this study support the idea that the sinking Sepik slab has influenced the evolution of the Eyre Basin, as proposed by Schellart and Spakman (2015). The numerical models in this study have produced evidence indicating dynamic subsidence in the Eyre Basin region from ~22-20 Ma, which correlates to geological evidence of Late Oligocene-Early Miocene subsidence (Alley, 1998). The Zahirovic et al. (2016) model, not previously explored in the context of dynamic topography, results in dynamic subsidence propagating further south than the other models. It is predicted that a 50 Ma collision model would propagate further south again, reaching the Lake Eyre region ~25-20 Ma, producing dynamic subsidence correlating even more closely with geologic evidence of ~25-20 Ma subsidence in the region. The work presented here however does not address the lithospheric heterogeneities, which may contribute or control the low elevations of Lake Eyre. The nature of Australia's continental character across the north-south Tasman Line (largely cratonic to the west, and Phanerozoic accreted terranes to the east), may amplify or focus the dynamic subsidence in the region of Lake Eyre, while the cratonic regions may have a greater lithospheric strength and be less affected by the mid-mantle Sepik slab. Future work will also require more detailed geodynamic modelling of continental lithosphere interactions with sinking slabs, as well as incorporating surface process models to capture the evolution of regional sedimentary depocenters such as Lake Eyre. In proposing a likely ~50 Ma collision timing of the Sepik terrane with the New Guinea margin, this study helps bridge tectonic reconstructions between Southeast Asia, the Indian Ocean, and the western Pacific. In addition, this study demonstrates the

strengths of using deep Earth constraints and modelling to help unravel the enigmatic geological histories of complex convergent margins.

## ACKNOWLEDGMENTS

Dr. Sabin Zahirovic, Dr. Rakib Hassan, and A/Prof Patrice Rey were supported by ARC grant IH130200012. This research was undertaken with the assistance of resources from the National Computational Infrastructure (NCI), which is supported by the Australian Government.

## REFERENCES

- Alley, N.F., 1998. Cainozoic stratigraphy, palaeoenvironments and geological evolution of the Lake Eyre Basin. *Palaeogeogr. Palaeoclimatol. Palaeoecol.* 144, 239–263.
- Artemieva, I.M., 2006. Global 1×1 thermal model TC1 for the continental lithosphere: implications for lithosphere secular evolution. *Tectonophysics* 416 (1), 245–277.
- Baldwin, S.L., Fitzgerald, P.G., Webb, E.W., 2012. Tectonics of the New Guinea region. *Annu. Rev. of Earth Planet. Sci.* 40, 495–520.
- Balmater, H.G., Manalo, P.C., Faustino-Eslava, D.V., Queaño, K.L., Dimalanta, C.B., Guotana, J.M., Ramos, N.T., Payot, B.D., Yumul, G.P., 2015. Paleomagnetism of the Samar Ophiolite: Implications for the Cretaceous sub-equatorial position of the Philippine island arc. *Tectonophysics* 664, 214–224.
- Becker, T., and Boschi, L., 2002. A comparison of tomographic and geodynamic mantle models: *Geochem. Geophys. Geosyst.* v. 3, 1003.
- Bower, D.J., Gurnis, M., Flament, N., 2015. Assimilating lithosphere and slab history in 4-D dynamic Earth models. *Phys. Earth Planet. Inter.* 238, 8–22.
- Butterworth, N., Talsma, A., Müller, R., Seton, M., Bunge, H.-P., Schubert, B., Shephard, G., Heine, C., 2014. Geological, tomographic, kinematic and geodynamic constraints on the dynamics of sinking slabs. *J. Geodyn.* 73, 1–13.
- Crowhurst, P.V., Hill, K.C., Foster, D.A., Bennett, A., 1996. Thermochronological and geochemical constraints on the tectonic evolution of northern Papua New Guinea. *Tectonic Evolution of Southeast Asia. Geological Society Special Publications* 106, 525–537.
- DiCaprio, L., Gurnis, M., Müller, R.D., 2009. Long-wavelength tilting of the Australian continent since the Late Cretaceous. *Earth Planet. Sci. Lett.* 278, 175–185.
- Dow, D.B., 1977. *A Geological Synthesis of Papua New Guinea 201.* Bureau of Mineral Resources, Australian Government Publishing Service.
- Flament, N., Gurnis, M., Williams, S., Seton, M., Skogseid, J., Heine, C., Müller, R.D., 2014. Topographic asymmetry of the South Atlantic from global models of mantle flow and lithospheric stretching. *Earth Planet. Sci. Lett.* 387, 107–119.
- Gaina, C., Müller, R.D., Royer, J.-Y., Symonds, P., 1999. Evolution of the Louisiade triple junction. *J. Geophys. Res.* 104, 12927–12940.
- Gee, J.S., Kent, D.V., 2007. Source of oceanic magnetic anomalies and the geomagnetic polarity time scale. *Treatise on Geophysics*, Vol. 5: Geomagnetism, pp. 455–507.
- Gurnis, M., Turner, M., Zahirovic, S., DiCaprio, L., Spasojevic, S., Müller, R.D., Boyden, J., Seton, M., Manea, V.C., Bower, D.J., 2012. Plate tectonic reconstructions with continuously closing plates. *Comput. Geosci.* 38 (1), 35–42.
- Hassan, R., 2016. *Dynamics of Mantle Plumes and their influence on Paleotopography.* PhD thesis, University of Sydney, NSW 2006.
- Hill, K.C., Hall, R., 2003. Mesozoic–Cenozoic evolution of Australia's New Guinea margin in a west Pacific context. *Geol. Soc. Aust. Spec. Publ.* 22, 265–289.
- Klootwijk, C., Giddings, J., Pigram, C.J., Loxton, C., Davies, H., Rogerson, R., Falvey, D., 2003. North Sepik region of Papua New Guinea: palaeomagnetic constraints on arc accretion and deformation. *Tectonophysics* 362, 273–301.
- Li, C., van der Hilst, R.D., Engdahl, E.R., Burdick, S., 2008. A new global model for Pwave speed variations in Earth's mantle. *Geochem. Geophys. Geosyst.* 9 (5), 21.
- Lus, W.Y., McDougall, I., Davies, H.L., 2004. Age of the metamorphic sole of the Papuan Ultramafic Belt ophiolite, Papua New Guinea. *Tectonophysics* 392, 85–101.
- Matthews, K.J., Müller, R.D., Wessel, P., Whittaker, J.M., 2011. The tectonic fabric of the ocean basins. *J. Geophys. Res.* 116 (B12), B12109.
- Müller, R.D., Seton, M., Zahirovic, S., Williams, S.E., Matthews, K.J., Wright, N.M., Shephard, G., Maloney, K.T., Barnett-Moore, N., Hosseinpour, M., Bower, D.J., Cannon, J., 2016. Ocean basin evolution and global-scale plate reorganization events since Pangea breakup. *Annu. Rev. Earth Planet. Sci.* 44.
- Pigram, C.J., Davies, H.L., 1987. Terranes and the accretion history of the New Guinea orogen. *Bureau Miner. Resour. J. Aust. Geol. Geophys.* 10:193–211.
- Queaño, K.L., Ali, J.R., Milsom, J., Aitchison, J.C., Pubellier, M., 2007. North Luzon and the Philippine Sea Plate motion model: Insights following paleomagnetic, structural, and age-dating investigations. *J. Geophys. Res.* 112.
- Schellart, W.P., Spakman, W., 2012. Mantle constraints on the plate tectonic evolution of the Tonga–Kermadec–Hikurangi subduction zone and the South Fiji Basin. *Aust. J. Earth Sci.* 59, 933–952.
- Seton, M., Whittaker, J.M., Wessel, P., Müller, R.D., DeMets, C., Merkuriev, S., Cande, S., Gaina, C., Eagles, G., Granot, R., 2014. Community infrastructure and repository for marine magnetic identifications. *Geochem. Geophys. Geosyst.* 15 (4), 1629–1641.
- Steinberger, B., Torsvik, T.H., 2008. Absolute plate motions and true polar wander in the absence of hotspot tracks. *Nature* 452 (7187), 620–623.
- Torsvik, T.H., Müller, R.D., van der Voo, R., Steinberger, B., Gaina, C., 2008. Global plate motion frames: toward a unified model. *Rev. Geophys.* 46 (3).
- Worthing, M.A., Crawford, A.J., 1996. The igneous geochemistry and tectonic setting of metabasites from the Emo Metamorphics, Papua New Guinea; a record of the evolution and destruction of a back-arc basin. *Mineral. Petrol.* 58 (1–2), 79–100.
- van der Meer, D.G., Spakman, W., van Hinsbergen, D.J.J., Amaru, M.L., Torsvik, T.H., 2010. Towards absolute plate motions constrained by lower mantle slab remnants. *Nat. Geosci.* 3, 36–40.
- Zahirovic, S., Matthews, K.J., Flament, N., Müller, R.D., Hill, K.C., Seton, M., Gurnis, M., 2016. Tectonic evolution and deep mantle structure of the eastern Tethys since the latest Jurassic. *Earth Sci. Rev.* 162, 293–337.
- Zhong, S., Zuber, M.T., Moresi, L., Gurnis, M., 2000. Role of temperature-dependent viscosity and surface plates in spherical shell models of mantle convection. *J. Geophys. Res.* 105 (B5), 11063.